

Hot-Wire Anemometry in Low-Density Flows

E. M. SCHMIDT* AND R. J. CRESCI†

Polytechnic Institute of Brooklyn, Farmingdale, N. Y.

The present paper deals with the use of hot-wire anemometry in obtaining quantitative flow data in the low-density, high-temperature regime. In conventional usage, high fluid temperatures result in decreased sensitivity due to structural limitations of the hot-wire probe. For intermittent testing, however, the wire supports remain at a low temperature, allowing the wire to be operated below the recovery temperature with high sensitivity. Since it is generally quite difficult to obtain a probe calibration in a low-density tunnel over a wide range of flow conditions, the wire heat balance is formulated, and solutions to the resulting boundary-value problem are obtained using numerical techniques. The coefficients in the equations (e.g., thermal conductivity, emissivity, accommodation coefficient, etc.) are all determined experimentally by static calibration. This permits a "dynamic calibration" curve to be generated outside of the wind tunnel for each probe.

Nomenclature

D	= wire diameter
E	= output voltage
I	= current, amps
k	= thermal conductivity
L	= wire length
M	= Mach number
p	= static pressure
Q_e	= Joule heating rate, Btu/sec
q	= heat-transfer rate; Btu/ft ² -sec
R_w	= wire resistance, Ω
\bar{R}	= average wire resistance, Ω
T	= temperature
\bar{T}	= average wire temperature
T_E	= support temperature
v	= velocity
x	= coordinate along wire
α	= accommodation coefficient
ϵ	= emissivity
λ	= mean free path
η	= coordinate normal to flat plate
ρ	= density
ξ	= coordinate along flat plate from leading edge

Subscripts

aw	= recovery conditions
c	= unheated probe conditions
fc	= forced convection
I	= intercept conditions
m	= measured conditions
0	= zero pressure
r	= probe surroundings
s	= stagnation conditions
t	= actual flow conditions
w	= conditions evaluated at wire temperature
∞	= freestream conditions

Presented as Paper 70-589 at the AIAA 5th Aerodynamic Testing Conference, Tullahoma, Tenn., May 18-20, 1970; submitted May 27, 1970; revision received March 22, 1971. This research was supported by the Air Force Office of Scientific Research under Contract F44620 71 C 0008, Project 9781 01, under the technical supervision of W. H. Smith, U. S. Air Force. The work reported here was based on part of a dissertation submitted by the first author to the faculty of the Polytechnic Institute of Brooklyn in partial fulfillment of the requirements for the degree of Doctor of Philosophy (Astronautics), 1969.

Index category: Research Facilities and Instrumentation.

* Formerly Research Associate; now Captain, U. S. Army Aviation Systems Command.

† Professor of Aerospace Engineering and Assistant Director, Gas Dynamics. Associate Fellow AIAA.

Introduction

THE measurement of detailed flow conditions in complex low-density, high-velocity flows has been performed qualitatively in the past; however, quantitative results have been generally unavailable. Some reasons for this lack of experimental information using standard measurement techniques have been the difficulty of interpretation of static pressure data, extremely low pressure levels, and low thermocouple recovery temperatures. Various new techniques have been proposed to overcome these difficulties, for example, electron beams, optical scattering, and hot-wire anemometry.

The constant-temperature anemometer has been utilized to some extent in the determination of local (mean) flow variables; however, the total temperatures and densities of interest at the Polytechnic Institute of Brooklyn (PIB) lie outside of the normally encountered range of laboratory usage. As a result, both measurement and data reduction techniques have been developed at PIB which are different from those previously utilized in the application of hot-wire anemometry.

When the flow temperature approaches the melting temperature of the wire, the anemometer output signal is very small, since the heat transfer is proportional to the difference between the recovery and the wire temperature. Hence, the sensitivity is quite poor. If the wire supports are externally cooled, the probe dimensions become too large, and, in addition, large amounts of wire end conduction are produced which overshadow the convection heating term in the over-all heat balance. Therefore, in order to maintain a constant mean wire temperature, large amounts of joule heating will be required to balance this end conduction. This causes a measurement problem, since it is desired to measure small variations (due to forced convection) in a large signal (due to end conduction).

In the present technique, the wire supports need not be externally cooled, since, for intermittent tunnel operation, the supports remain at their initial ambient temperature. This facilitates the design of the probe and also permits its size to remain quite small. The problem of end conduction, however, remains. Attempts have been made in the past to correct for the end conduction,⁶⁻⁸ but these techniques are inapplicable in the present case. Previous results were derived for steady-state tunnel conditions wherein the wire supports have reached their equilibrium (or recovery) temperature. As a result, the mean wire temperature and the support temperature are relatively close to each other. In the current mode of operation, the support temperature is only a small fraction of the mean wire temperature, thereby necessitating

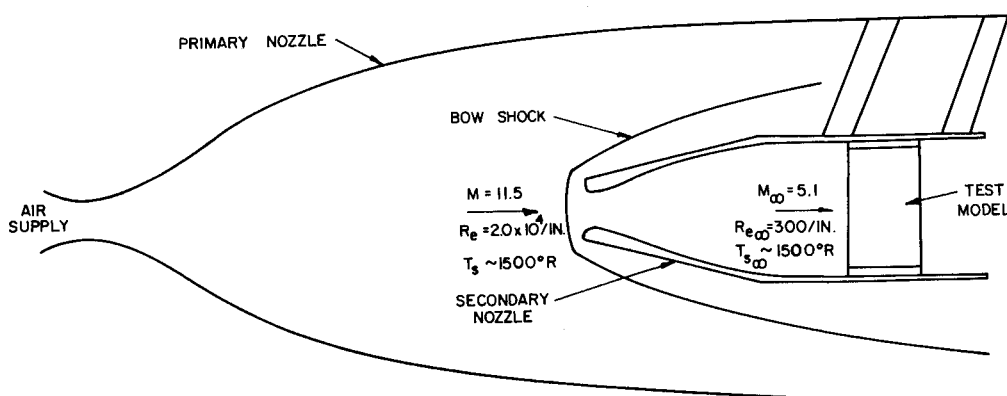


Fig. 1 Schematic of test setup.

a different correction scheme. The radiation correction considered in Refs. 9 and 10 also is not possible, since it is based on a linearization of the difference between the maximum and mean wire temperatures; this difference is also quite large in the present measurement technique.

The approach taken here is to formulate the standard wire heat-transfer relation and obtain solutions to the resulting boundary-value problem using finite-difference techniques. The coefficients in the equation (e.g., thermal conductivity, emissivity, accommodation coefficient, etc.) are all determined experimentally by static calibration. This permits a "dynamic calibration" curve to be generated outside of the wind tunnel for each probe. This significantly enhances the utility of the hot-wire system, since it is generally quite difficult to obtain a probe calibration in a low-density tunnel over a wide range of flow conditions. The wind-tunnel facility available at PIB for low-density testing is shown schematically in Fig. 1. This technique was developed by Ferri¹ and consists of a secondary nozzle placed inside a hypersonic tunnel; because of the large drop in stagnation pressure, extremely low densities are achieved therein. For the conditions shown here, the mean free path is on the order of 0.03 in.; the freestream Reynolds number is 300/in., and the test section Mach number is 5.1. The tunnel is an intermittent blowdown type, which, although it has some limitations, is ideally suited for the measurement technique described here.

In the following sections, the heat-balance analysis and the data acquisition and reduction procedures are presented. Typical flat-plate profiles of density and velocity are also shown as an example of the data obtainable utilizing the present technique.

Heat-Transfer Analysis for the Hot Wire

Boundary-Value Problem

The constant-temperature hot wire is utilized in the present survey to measure the local mass flow rate ρv and recovery temperature. To interpret the output of the wire, it is necessary to consider the particular conditions under which it is operating, for example, 1) low-density flow (the flow is free molecular based on wire diameter), 2) intermittent flow (2–3-sec test time), 3) relatively short wire length ($L/D \approx 200$ –500), 4) unheated wire supports, and 5) recovery temperature $\approx 2000^\circ\text{R}$.

These factors combine to create a situation in which it is difficult to extract valid, coherent data using previously established techniques. Examination of the convective heat-transfer term and consideration of certain wire properties will demonstrate the reason for this. The forced-convection heat transfer between a circular cylinder and the flow in which it is immersed is

$$q_{fc} \sim (\rho v)^n [T_w - T_{aw}]$$

To optimize the sensitivity for given flow conditions requires

the adjustment of the mean wire temperature T_w such that the temperature difference is maximized. The standard technique is to operate the wire at a mean temperature considerably higher than the flow recovery temperature. However, for high values of T_{aw} , difficulties are encountered, since the amount that the wire temperature can be increased is limited by structural considerations. At high temperatures, the wire is susceptible to various failures, among which are creep, plastic deformation under aerodynamic loading, and even melting.

In order to operate in high-enthalpy flows, cooled film probes have been developed as described in Ref. 2–4. These hot films are internally cooled, either by gas or water, which enables operation at film temperatures below the recovery temperature, since the heat balance is not just between the film and the flow, but rather among the film, the flow, and the coolant. In the present case, the cold supports act as a heat sink for the hot wire in the same manner as the coolant does for the hot film. Thus, it is possible to operate the hot wire at average temperatures below the recovery temperature and obtain sensitivities that would not be possible at higher temperatures because of probe failure. It must be noted that this type of operation without artificial support cooling is practical only for short test times, such that the low rates of convective heat transfer do not heat the supports appreciably during the test.

Consideration also must be given to the effect on the anemometer output of the temperature distribution along the wire due to the short length and cold supports. The temperature will vary about the mean wire temperature, reaching a maximum at the wire center and decreasing to the support temperature at the wire-support junction. Stalder et al.⁵ have shown that for free molecular flow the two-dimensional forced-convection heat transfer from a cylinder normal to the flow is

$$q_{fc} \sim \rho v (T_w - T_{aw})$$

If it is assumed that this may be applied locally along the wire, it is immediately apparent that the magnitude of the convective heat transfer will vary along the wire in direct proportion to the local wire temperature. Under the influence of a variation in the flow environment, the anemometer amplifiers could maintain a constant mean wire temperature, but not a constant temperature distribution because of the nonuniform distribution of heat transfer along the wire. Since the magnitude of end-conduction heat transfer is dependent upon the wire temperature distribution (in particular dT_w/dx at the wire-support junction), variation in the temperature distribution with flow changes will cause a variation in the magnitude of end-conduction heat transfer. This must be accounted for in the data interpretation scheme.

The energy balance for an elemental length of wire (Fig. 2) is considered. It is assumed that the wire has a small diameter and, in addition, that an equilibrium state has been established such that there is no radial variation in temperature. Considering heat transfer into the wire as positive, the

energy balance may be expressed as

$$(q_x - q_{x+dx})(\pi D^2/4) + (q_{fc} - q_r)\pi D dx + Q_e = 0 \quad (1)$$

which reduces to

$$d/dx [k(dT_w/dx)](\pi D^2/4) + [q_{fc} - q_r]\pi D + (Q_e/dx) = 0 \quad (2)$$

where $k(T)$ and all other constants are evaluated experimentally.

Now define

$$\bar{x} = 2x/L \quad (3)$$

Then for

$$-L/2 \leq x \leq L/2 \quad -1 \leq \bar{x} \leq 1$$

Assuming that the wire radiates as a gray body, i.e., independent of wavelength, the radiation term becomes

$$q_r = 0.48 \times 10^{-12} \epsilon [T_w^4 - T_r^4] \quad (4)$$

Joule heating is expressed as

$$Q_e = EI = I^2 R_w$$

For an element of length dx of wire, the resistance is

$$R = (R_e/T_e L) dx T_w$$

It should be noted that this simple relation is true for platinum wire; in general, however, the more exact relation

$$R = [R_{ref} + AT_w]dx/L$$

should be utilized. Assuming the wire to be composed of a series of elemental resistances in series, one obtains

$$Q_e = I^2 (R_e/T_e L) dx T_w \quad (5)$$

Furthermore, assuming the flow to be two-dimensional for the length of the wire, and using the results of Stalder,⁵ the expression for convective heat transfer in free molecular flow where the freestream Mach number is greater than approximately three is

$$q_{fc} = 6.85 \alpha \rho v [T_{aw} - T_w] \quad (6)$$

Combining terms,

$$\frac{\pi D^2}{L^2} \left[\frac{dk}{dT_w} \left(\frac{dT_w}{d\bar{x}} \right)^2 + k \frac{d^2 T_w}{d\bar{x}^2} \right] + 6.85 \alpha \pi D \rho v \times [T_{aw} - T_w] - 0.48 \times 10^{-12} \pi D \epsilon [T_w^4 - T_r^4] + 0.948 \times 10^{-3} I^2 \frac{R_e T_w}{T_e L} = 0$$

with the boundary conditions

$$dT_w/d\bar{x} = 0 \quad \text{at } \bar{x} = 0 \quad T_w = T_e \quad \text{at } \bar{x} = \pm 1$$

It is now desired to solve the boundary-value problem for the wire temperature distribution, given the wire geometry and physical properties. By selecting a flow with a particular set of properties and varying the input current, the temperature distribution at each current may be solved for. Using the following relation:

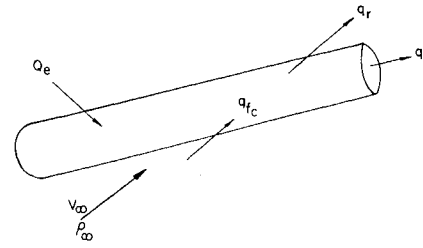
$$\bar{T}_w = \int_0^1 T_w d\bar{x}$$

the mean wire temperature is obtained, and the mean wire resistance is

$$\bar{R}_w = (R_e/T_e) \bar{T}_w$$

Since the anemometer reads the voltage across a Wheatstone bridge, the theoretical output can easily be expressed in terms of this resistance using

$$E = I(\bar{R}_w + 40)$$



$$Q_e = \text{JOULE HEATING} = I^2 R = E^2/R$$

$$q_{fc} = \text{FORCED CONVECTION} \sim \rho \omega v_\infty (T_{aw} - T_w)$$

$$q_r = \text{RADIATION COOLING} \sim \epsilon (T_w^4 - T_r^4)$$

$$q = \text{CONDUCTION COOLING} \sim \left(k \frac{\partial T}{\partial x} \right)_{\text{SUPPORT}}$$

$$\frac{E^2}{R} \sim \frac{q_r + q}{E_0^2/R} + \rho v (T_w - T_{aw})$$

$$\frac{E^2 - E_0^2}{R} \sim \rho v (T_w - T_{aw})$$

Fig. 2 Heat balance on hot-wire element.

where a 40- Ω resistor is in series with the probe for the particular anemometer used. Thus, for a given wire and set of flow conditions, a plot of the voltage E necessary to maintain the wire at a given resistance \bar{R}_w is obtained. By varying the input flow conditions, a family of these curves is obtained and may be cross-plotted to examine the theoretical hot-wire behavior. The finite-difference scheme and program are given in Ref. 11, and the technique of obtaining the various physical constants required as inputs is explained in the Appendix.

Solutions to the Boundary-Value Problem

Although various probe geometries were utilized and a series of computations performed for each of these, cf. Ref. 11, for the present purposes a platinum wire probe is considered with the following characteristics: $L = 0.1$ in., $D = 0.0005$ in., $R_e = 2.5 \Omega$, and $T_e = 530^\circ\text{R}$. The effect of variation of the flow properties, in particular the mass flow and stagnation temperature, upon the wire response is now examined. Prior to this examination, however, it is beneficial to consider the wire response at zero pressure, that is, with zero convective heat transfer.

The behavior of the hot wire in the absence of all convection effects is determined by the energy balance among joule heating, end conduction, and radiation. The solution of the governing equation is relatively simple by numerical techniques, and the results of the finite-difference computation are plotted in Fig. 3. The plot shows the mean wire resistance vs the voltage necessary to maintain the wire at this resistance. This voltage corresponds to the output of the anemometer which is related to the voltage drop across the wire. The range in mean wire resistance, 2.5–10 Ω , is limited at the lower end by the cold resistance and at the upper end by structural limitations. Plotted on this figure are the data obtained from several of these zero-pressure calibrations. It should be noted that the thermal conductivity of the wire is assumed to correspond to the value providing the minimum deviation from the experimental data, cf. Appendix. The zero forced-convection curve is important in that it forms the basis for the technique utilized to determine the flow recovery temperature.

The recovery temperature measurement technique used is similar to that of Laurmann,^{6,9} wherein the recovery temperature is taken to correspond to the wire resistance measured when no heating current is passing through the system. The wire used by Laurmann was for all practical purposes in-

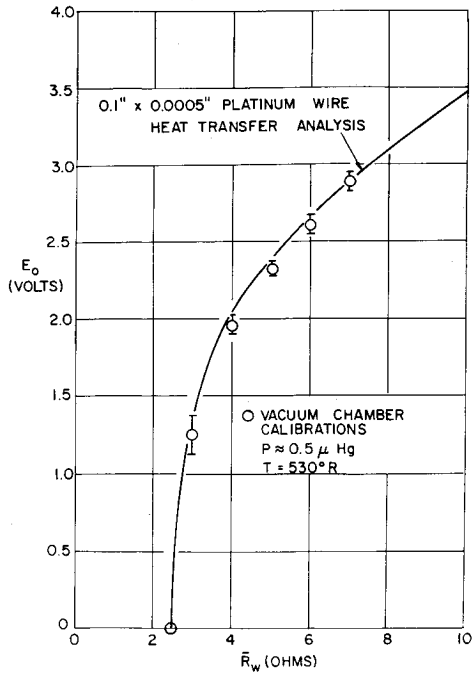


Fig. 3 Zero-convection heat-transfer analysis output voltage vs mean wire resistance.

finite in length; thus the power supplied to the wire provided Joule heating to balance cooling due to forced-convection heat transfer. Examination of the heat-transfer relation for this case shows that the wire temperature is equal to the recovery temperature when the power supplied to the wire is essentially zero.

For a finite-length wire, however, the effect of end conduction must be considered. When the mean wire temperature is equal to the recovery temperature, the power supplied to the wire will not be zero, even though there is no forced-convection heat transfer. This is because power is required to balance end conduction cooling. Extending Laurmann's technique, Todisco and Pallone¹²⁻¹⁴ developed a method applicable to the finite-length, cool-support hot wire. Utilizing

a shock tunnel and a constant-temperature anemometer, the wire output was measured before each test. This output represents the power necessary to maintain the wire at a selected resistance, balancing cooling due to end conduction and radiation. The criterion for zero forced-convection heat transfer then requires the output during the test to be equal to the output prior to the test. When this condition is achieved, the mean wire temperature is said to equal the recovery temperature. To select the exact operating resistance at which this will occur is difficult; therefore, the wire is operated at several resistances near the recovery value and the results extrapolated. This method assumes that the magnitudes of end conduction prior to and during the test are identical. However, in order to utilize this technique at very low densities, consideration must be given to the variation in

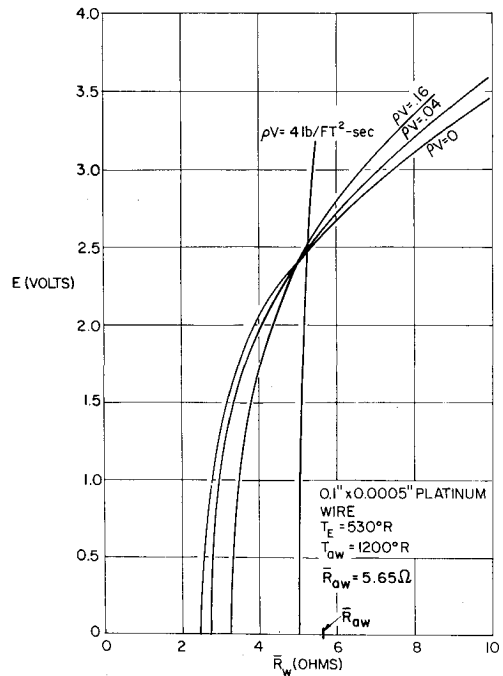


Fig. 4b Heat-transfer analysis results for $T_{aw} = 1200^{\circ}\text{R}$.

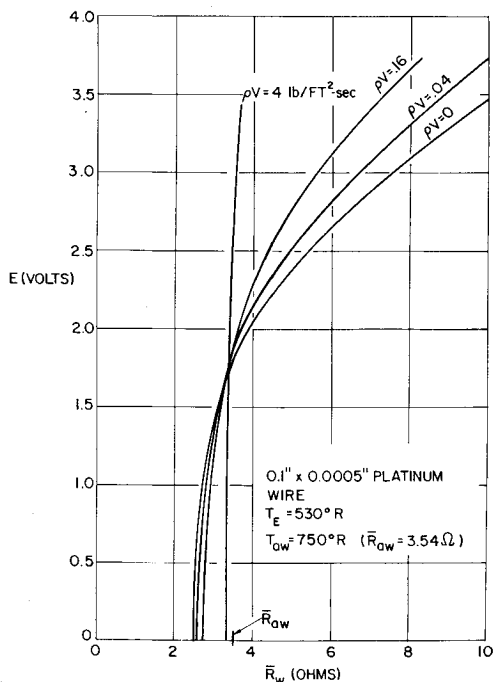


Fig. 4a Heat-transfer analysis results for $T_{aw} = 750^{\circ}\text{R}$.

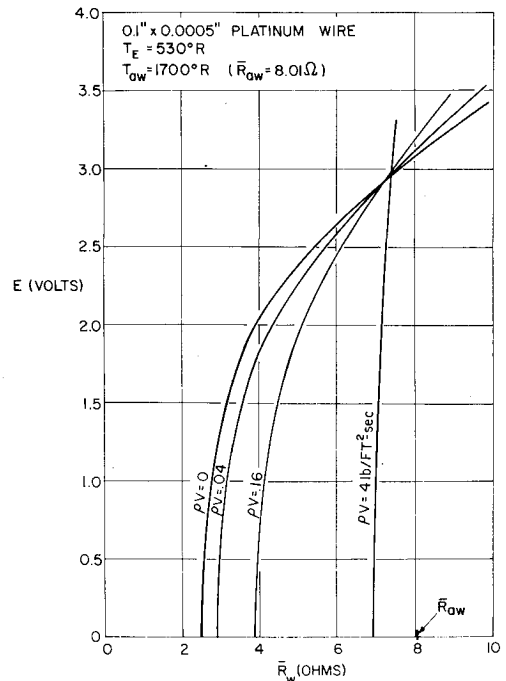
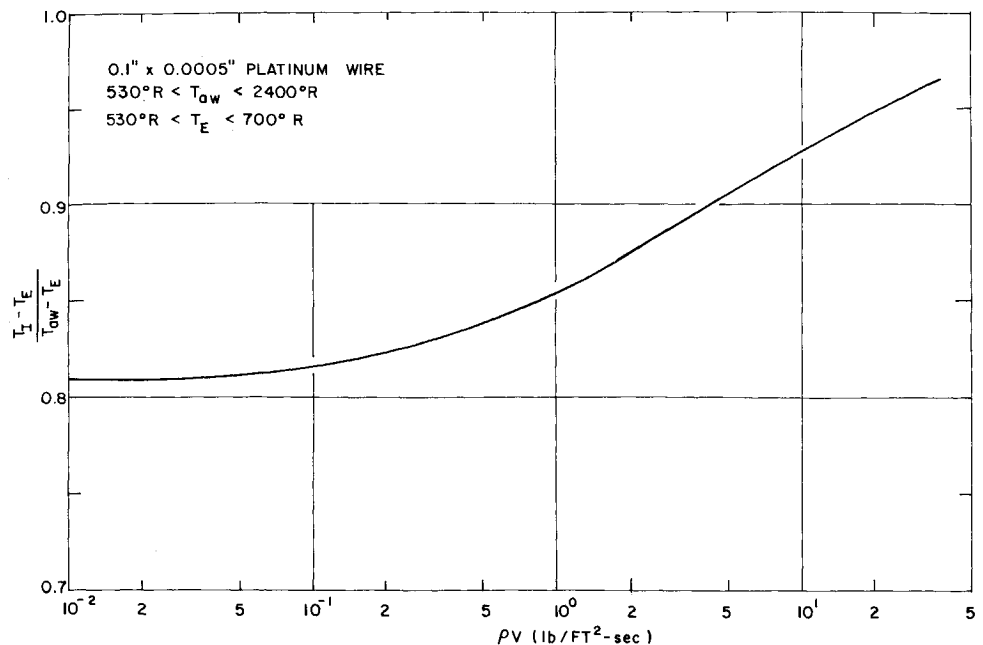


Fig. 4c Heat-transfer analysis results for $T_{aw} = 1700^{\circ}\text{R}$.

Fig. 5 Intercept temperature vs mass flow.



temperature distribution along the wire and the variation in end conduction resulting therefrom. The zero pressure calibration (Fig. 3) corresponds to the zero convective heat-transfer condition that is required to determine the recovery temperature. However, since the magnitudes of end conduction between the flow and no-flow conditions are not equal, the effect of this on the resulting intercept must be considered.

To examine this effect, numerical computations were made, including the forced-convection heat-transfer term. The results of these computations are plotted in Figs. 4a-4c for different values of the recovery temperature. Several values of mass flow are included in each plot to illustrate the effect of increasing mass flow upon the response curve. Also included on each plot is the zero pressure response curve, which is the same in each case, since it is independent of mass flow and recovery temperature.

The recovery temperature, according to previous methods, should correspond to the value of resistance obtained at the intersection of the flow and no-flow curves. From the figures shown, this intercept point is readily apparent. As the recovery temperature increases, the intersection point moves to higher values of resistance. Examination of the value of mean wire temperature corresponding to the intercept resistance, however, shows that in each case the temperature T_i is considerably less than the recovery temperature. The deviation is due to the difference in magnitude of end conduction between the flow and no-flow conditions.

An additional effect that must be considered is the variation of the intercept location with mass flow. Figures 4a-4c show that, as the mass flow increases, the intersection location approaches the recovery temperature. In the limiting case of infinite mass flow, the wire temperature distribution would be practically uniform at the recovery temperature level. For intermediate values of the mass flow, the intercept data for various adiabatic wall temperatures has been correlated according to the difference in recovery and support temperature. This parameter is plotted in Fig. 5, where it is seen that for low values of the mass flow the ratio is relatively constant; thus knowledge of the exact value of ρv is not necessary for application of the correction in this range. It is also observed that, for $\rho v \rightarrow \infty$, the correction parameter approaches unity as discussed previously.

Another factor that affects the intercept resistance is the support temperature. As the mean wire operating temperature is varied, the support temperature varies. To determine this variation with wire operating temperature, or re-

sistance, a special probe was constructed with a thermocouple mounted within 0.002 in. of the wire-support junction. The probe, which is discussed in detail in Ref. 11, was fabricated to the same dimensions as the standard probe. The results of the survey over a range in operating resistance showed a corresponding variation in support temperature from 530° to 620°R. With this range of support temperatures as a guide, the boundary conditions in the computations may be selected to yield a corresponding set of values. This probe also was used during actual tests, and the same variation in support temperature occurred, indicating that the aerodynamic heating of the supports was negligible.

The variation in the zero pressure curves (Fig. 6) shows how the support temperature affects the output. As the support temperature increases, the zero power resistance increases, whereas the power necessary to maintain the wire at a given

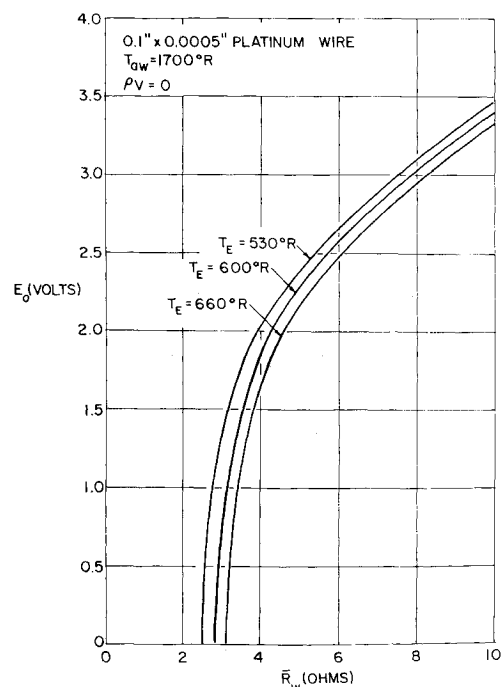


Fig. 6 Variation in zero-convection results with changing support temperature.

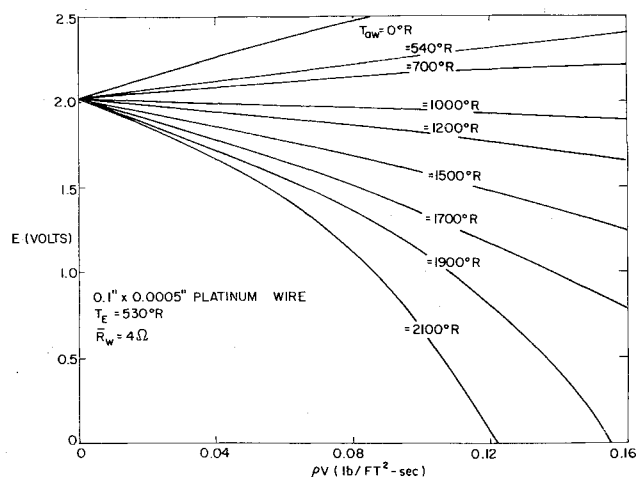


Fig. 7 Output voltage vs mass flow for $\bar{R}_w = 4\Omega$.

resistance decreases. Both of these effects could be anticipated. At zero power with zero forced-convection heat transfer, the wire will assume the temperature of the supports by conduction; thus the zero power resistance shifts according to the linear resistance-temperature relation. The decrease in voltage at a fixed operating resistance is proportional to the decrease in end-conduction heat transfer caused by the decrease in temperature difference between the wire and the supports with increasing support temperature. To determine how these shifts will affect the intercept temperature, computations were made including the forced-convection term.

A constant value of recovery temperature equal to 1700°R was selected for this study, as this is roughly the temperature obtained in the secondary nozzle facility at PIB. The results of these computations show trends similar to those obtained for the constant support temperature case; moreover, the parameter presented in Fig. 5, which includes the support temperature variation, is found to be valid independent of support temperature.

Since there are appreciable shifts in output voltage at a fixed resistance with variation in support temperature, the validity of crossplots at fixed support temperature to obtain variations in output with mass flow is not strictly applicable, and yet qualitative results will indicate the data trends. Using the curves for a value of $T_e = 530^\circ\text{R}$, Figs. 4a-4c will yield crossplots that reflect the behavior of the output with variations in flow parameters. This is presented in Fig. 7, for an operating resistance of 4Ω . This figure presents the variation in output with mass flow at different values of recovery temperature. The zero mass flow intercept is identical for each curve and equal to the zero pressure (convection) output voltage. The slope of the curves changes from positive to negative when the recovery temperature is such that the intercept temperature is equal to the mean wire temperature.

In order to obtain a calibration of the hot wire in the tunnel, it is desirable to vary as few flow parameters as possible and still obtain a comprehensive calibration. An attempt to reproduce Fig. 7 through actual test calibration is obviously impractical. Thus, it is necessary to obtain a correlation parameter that can be used to predict these curves. Since the results of the heat-transfer analysis indicate that the intercept temperature is a basic property obtained, a plot is made of output voltage vs the parameter $\rho v(T_i - T_w)$, Fig. 8. The resulting correlation curve has a narrow band within which the uncertainty is minimal. Utilization of this parameter in calibration of the wire will enable a calibration to be made at one value of intercept temperature and utilized for all other values of intercept temperature greater than the mean wire temperature. Refinement of this correlation curve can be

accomplished, including the effects of support temperature variation if desired.

Experimental Technique

Hot-Wire Probes

Since no two hot-wire probes are exactly alike, each probe must be statically calibrated and great care taken to insure that the calibrations remain valid throughout the probe life.

Three calibrations are performed on each wire: a resistance-temperature calibration, a zero-pressure calibration, and a mass flow check calibration. The resistance-temperature calibration is used to check the linearity of the resistance-temperature relation over the range of wire temperatures of interest. The probe is placed in an oven and the resistance monitored by the anemometer, thus providing the coefficient used in the relation

$$\bar{R}_w = (R_e/T_e)\bar{T}_w$$

The resistance-temperature relation for the wire is also essential for the determination of the recovery temperature. For all wires of a given geometry surveyed, the coefficient R_e/T_e is found to be within 4% of the manufacturer's specifications.

The zero-pressure calibration is made in a specially constructed vacuum system, consisting of mechanical pumps for roughing and holding and a diffusion pump with the capability of evacuating the test container, a 10-in. bell jar, to less than $0.1 \mu\text{Hg}$. For the short wires used, the dominant heat-transfer term at this pressure is due to end conduction. In fact, the heat-transfer analysis shows no discernable effect of pressure (free convection) for pressures up to $1 \mu\text{Hg}$; thus the vacuum system is considered to present effectively a zero pressure environment to the hot-wire probe. The probe is operated over the range of resistances of interest and the output recorded as in Fig. 3. Since at each operating resistance the support temperatures attain a different equilibrium value, sufficient time (2-5 min) is allowed between successive readings to assure that this equilibrium temperature is achieved. The wire is joined to the probe supports using either soft or silver solder; therefore, to eliminate any error that operating the wire at elevated temperatures may have upon the solder junction, the zero pressure calibration is repeated over the full range of operating resistances until consistent results are obtained for two successive calibrations.

Having obtained the zero-pressure calibration, the probe may be used to determine the intercept temperature without further calibration, as follows. The hot wire is operated at several different values of resistance; the operating resistance that yields an output voltage equal to the zero-

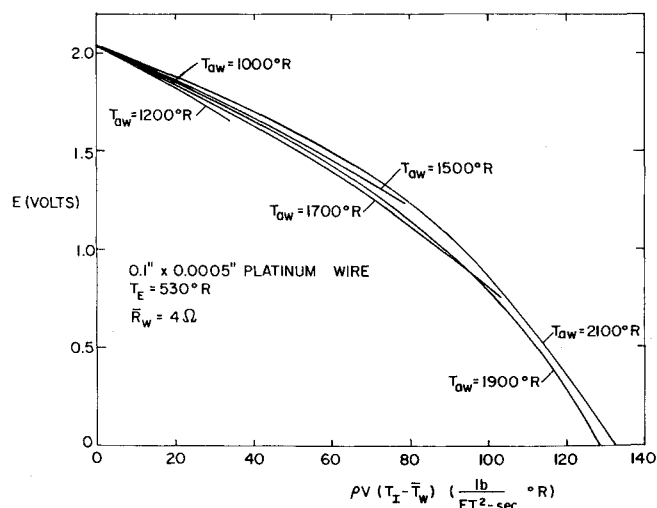


Fig. 8 Output voltage vs $\rho V(T_i - T_w)$ for $\bar{R}_w = 4\Omega$.

pressure voltage is the intercept resistance, from which the intercept temperature at the particular point in the flowfield is found. To simplify the extrapolation necessary to find the intercept resistance, the difference in power between the test and zero pressure calibration is plotted for each operating resistance. In terms of this parameter, the intercept resistance occurs at the zero-power intercept, cf. Fig. 9. The intercept temperature and the results of the heat-transfer analysis (Fig. 5) will then yield the recovery temperature. Then to obtain the flow stagnation temperature, the recovery ratio T_{aw}/T_s can be found using the results of Ref. 5.

To determine the mass flow, the hot-wire probe is then check-calibrated in the tunnel. This is done in the free-stream of the secondary nozzle. Since the freestream velocity and stagnation temperature are fixed, the stagnation pressure is varied over a range sufficient to obtain a comprehensive calibration. Figure 10 presents the results of one such calibration taken over a range in mainstream stagnation pressure from 100–400 psi. The calibration is taken at a fixed wire resistance and the resulting output voltage plotted vs the mass flow; a comparison with the results of the analysis including the effect of support temperature variation is shown.

To obtain local mass flow data, the hot wire is traversed through the region of interest at the same wire resistance as in the calibration. Using the calibration curve, the parameter $\rho v(T_i - T_w)$ may be found corresponding to each output voltage. Knowing the intercept temperature, the temperature difference $(T_i - T_w)$ is defined, and at each point the measured mass flow $(\rho v)_m$ is then determined.

Data Reduction Technique

The hot-wire data available directly from measurements and calibration consists of uncorrected mass flow and actual recovery temperature. In order to develop a consistent set of flow properties, these measurements must be altered to account for effects of local Mach number, when the Mach number is less than 3.0.

Stalder et al.⁵ present the following relation for free molecular forced-convection heat transfer:

$$q_{fc} = [g(s)/s](\rho v)[T_{aw} - T_w]$$

where $g(s)/s$ is a function of Mach number which is defined and tabulated in the aforementioned reference. Thus, to utilize the previous calibration (at $M = 5.1$) at lower Mach

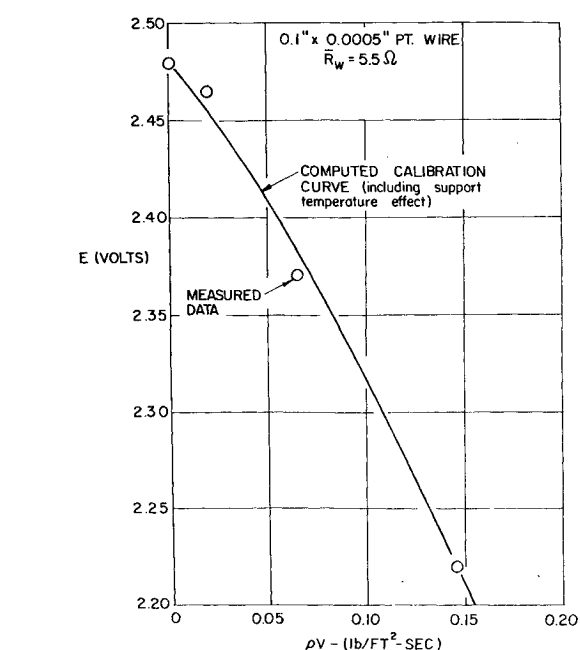


Fig. 10 Mass flow calibration check in tunnel.

numbers, an equivalent mass flow must be found which produces a voltage output equal to that produced by a particular value of mass flow on the calibration curve. Use is made of the fact that the forced-convection heat transfer in both cases is the same; therefore,

$$[g(s)/s](\rho v)_t(T_{aw} - T_w) = 10.72(\rho v)_m(T_{aw} - T_w)$$

Thus,

$$(\rho v)_t = [10.72s/g(s)](\rho v)_m$$

where t refers to the actual conditions, and m refers to the measured conditions.

Although $g(s)/s$ is virtually independent of Mach number for $M > 3.0$, it is quite sensitive for lower Mach numbers. In order to obtain ρv at low Mach numbers, therefore, it is necessary to obtain a pitot pressure measurement that will (in conjunction with the raw ρv data) permit evaluation of the local Mach number. The local mass flow and stagnation temperature can then be computed readily.

Concluding Remarks

Typical plots of the final data obtained on a sharp flat plate at distances of roughly 80 and 65 mean free paths from the leading edge are shown in Fig. 11. Mass flow profiles are compared to the theoretical predictions of Ref. 15. Flow structure both in the viscous and shock layer is evident, as well as a region of velocity slip at the plate surface. The analysis has subsequently been shown to overpredict the peak density as found in the experiments.

Although the study of supersonic flows at low densities requires extreme care in the selection and utilization of surveillance tools, the technique developed here appears to yield reasonable results. Using a hot-wire probe and a pitot probe, complete flow properties are attainable; however, the test conditions in the present survey were such as to make certain corrections minimal. Typically, three tests were required to obtain a satisfactory intercept temperature T_i .

The utilization of the hot-wire probe in this survey is rather unique. Since the test duration is short and convective heating rates are low, the wire supports remain essentially at the ambient temperature during the test. This provides a heat sink for the wire which simulates the operating char-

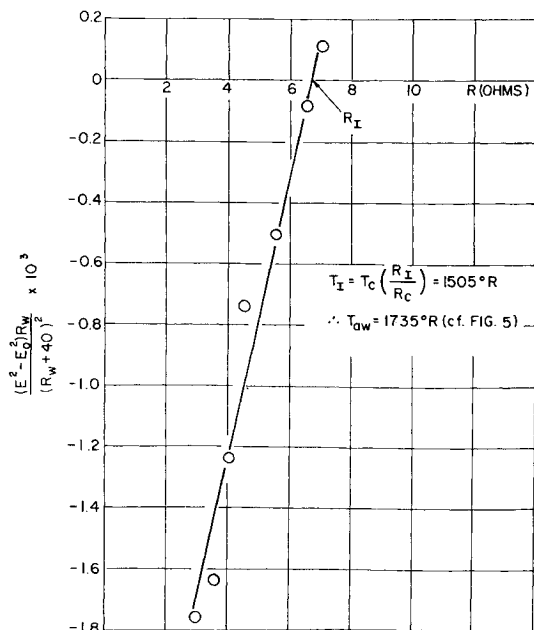


Fig. 9 Determination of recovery temperature.

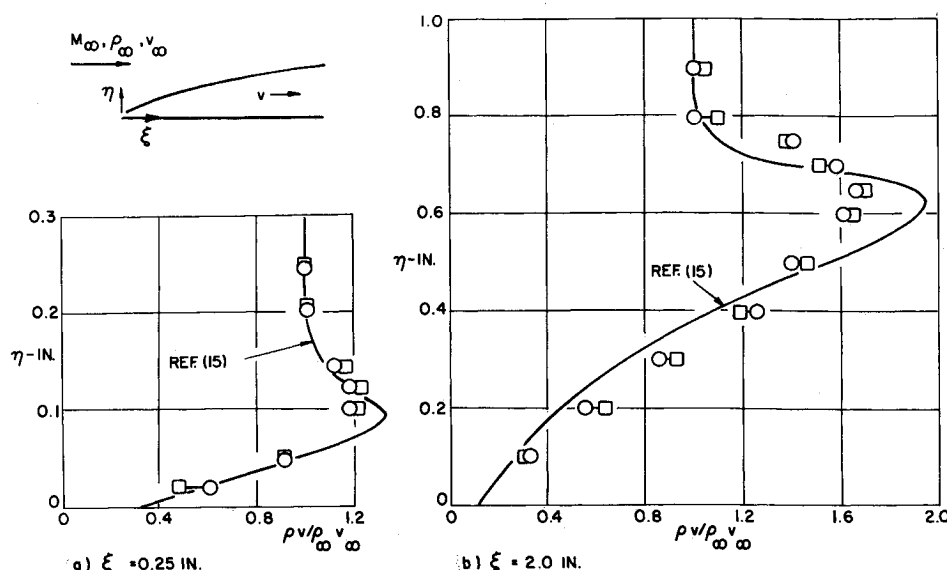


Fig. 11 Mass flow profiles on flat plate.

acteristics of a cooled probe. By careful analysis of the wire response to different fluid temperatures and mass flows, a probe has been designed which operates at mean wire temperatures below the recovery temperature. However, care must be taken to insure consistency of all controllable variables influencing the probe performance, including support temperature, wire soundness and calibration, and test condition uniformity. Since this is no more than standard procedure for any hot-wire operation, the difficulties are not insurmountable.

Appendix: Evaluation of Physical Constants of Hot-Wire Material

It is important to evaluate the physical properties of the wire material from which the probe is constructed, since the wire manufacturer does not generally supply sufficient information to perform the heat balance computation accurately, and handbook values are not exactly valid, since they correspond to pure, clean specimens under controlled atmospheric conditions. As a result, the physical characteristics of each wire sample were determined as follows.

Emissivity

Examination of the heat balance equation indicates that one method of determining the emissivity is to construct a wire with a very long length-to-diameter ratio. For this configuration, the conduction term drops out. If the probe environment is at a very low pressure, the convection term also will be zero. Knowing the resistance temperature relation, one can then determine the emissivity by setting the wire at different temperatures electrically and measuring the applied voltage. In this manner, all of the electrical heating is dissipated by radiation to the surroundings, and the effective emissivity can be computed. This was done experimentally in an evacuated bell jar pumped down to a pressure less than 0.1μ . A wire with a length-to-diameter ratio of approximately 10^5 was used. As seen in the heat-balance equation, this represents a coefficient for the conduction term on the order of 10^{-10} , which yields negligible end conduction. The results of this measurement produced a value of the measured emissivity of roughly $2\frac{1}{2}$ times the handbook values. This is probably caused by the change in surface properties due to wire heating, collection of dust, and erosion, whereas the handbook values are all given for highly polished, clean specimens.

Thermal Conductivity

The thermal conductivity can now be obtained by again inserting the hot-wire probe into a bell jar at zero pressure and comparing the measurements to the computed voltage vs resistance characteristics for various values of the conductivity, since the other terms in the equation are now known. This was done, and it was found possible to match the measured data with the computed values for the specified boundary conditions if the effect of the support temperature variation is included. The thermal conductivity measured in this manner is approximately 20% higher than that given in the various handbooks. The cause for this variation may be due to slight impurities in the wire manufacturing process due to alloying elements added for strength and also due to the annealing process that occurs as the wire is alternately heated and cooled.

Accommodation Coefficient

There remains only one coefficient as yet undetermined; this is the accommodation coefficient, which is related to the free convection, or forced convection, term. Having determined the three other terms in this equation, α can be found by heating the wire in the bell jar and measuring the voltage output at different ambient pressures. The values of α thereby determined is 0.85, which has been used previously. Now that all of the coefficients are known, the numerical solution to this equation can be used to obtain a calibration curve. One merely replaces the free convection term, which is proportional to static pressure, by the forced convection term, which is proportional to mass flow.

References

- ¹ Ferri, A., Zakkay, V., and Ting, L., "Blunt Body Heat Transfer at Hypersonic Speed and Low Reynolds Number," *Journal of the Aerospace Sciences*, Vol. 28, No. 12, Dec. 1961, pp. 962-972.
- ² Blackshear, P. L. and Fingerson, L., "Rapid-Response Heat Flux Probe for High Temperature Gases," *ARS Journal*, Vol. 32, No. 11, Nov. 1962, pp. 1709-1715.
- ³ McCroskey, W. J., "Density and Velocity Measurements in High Speed Flows," *AIAA Journal*, Vol. 6, No. 9, Sept. 1968, pp. 1805-1808.
- ⁴ McCroskey, W. J., Bogdonoff, S. M., and McDougall, J. G., "An Experimental Model for the Sharp Flat Plate in Rarefied Hypersonic Flow," *AIAA Journal*, Vol. 4, No. 9, Sept. 1966, pp. 1580-1587.
- ⁵ Stalder, J. R., Goodwin, G., and Creager, M. O., "A Com-

parison of Theory and Experiment for High-Speed Free-Molecule Flow," Rept. 1032, 1951, NACA.

⁶ Laurmann, J. A. and Ipsen, D. C., "Use of a Free Molecule Probe in High Speed Rarefied Gas Flow Studies," TR HE-150-146, April 1957, Univ. of California, Berkeley.

⁷ Dewey, C. F., Jr., "Hot Wire Measurements in Low Reynolds Number Hypersonic Flows," *ARS Journal*, Vol. 31, No. 12, Dec. 1961, pp. 1709-1718.

⁸ Staylor, W. F. and Morrisette, E. L., "Use of Moderate-Length Hot Wires to Survey a Hypersonic Boundary Layer," *AIAA Journal*, Vol. 5, No. 9, Sept. 1967, pp. 1698-1700.

⁹ Laurmann, J. A., "The Free Molecule Probe and Its Use for the Study of Leading Edge Flows," *The Physics of Fluids*, Vol. 1, No. 6, Nov.-Dec. 1958.

¹⁰ Vrebalovich, T., "Heat Loss and Recovery Temperature of Fine Wires in Transonic Transition Flows," *Rarefied Gas Dynamics*, edited by C. L. Brundin, Vol. 2, Academic Press, New York, 1967, pp. 1205-1219.

¹¹ Schmidt, E. M., "Merged Layer Flow in an Interior Corner," Ph.D. thesis, June 1969, Polytechnic Institute of Brooklyn.

¹² Todisco, A., Pallone, A., and Heron, K., "Hot Wire Measurements of the Stagnation Temperature Field in the Wake of Slender Bodies," RAD-TM 64-32, July 1964, Avco Corp., Wilmington, Mass.

¹³ Todisco, A. and Pallone, A., "Near Wake Flow Field Measurements," *AIAA Journal*, Vol. 3, No. 11, Nov. 1965, pp. 2075-2080.

¹⁴ Todisco, A. and Pallone, A., "Measurements in Laminar and Turbulent Near Wakes," AIAA Paper 67-30, New York, 1967.

¹⁵ Rudman, S. and Rubin, S. G., "Hypersonic Flow Over Slender Bodies with Sharp Leading Edges," *AIAA Journal*, Vol. 6, No. 10, Oct. 1968, pp. 1183-1890.

Vortex Computation by the Method of Weighted Residuals Using Exponentials

HARTMUT H. BOSSEL*

University of California, Santa Barbara, Calif.

A method of weighted residuals for the computation of rotationally symmetric quasi-cylindrical viscous incompressible vortex flow is presented. The method approximates the axial velocity and circulation profiles by series of exponentials having $(N + 1)$ and N free parameters, respectively. Exponentials are also used as weighting functions. Formal integration results in a set of $(2N + 1)$ ordinary differential equations for the free parameters. The governing equations are shown to have an infinite number of discrete singularities. Sample solutions for different swirl parameters and three typical vortex flows (initially uniform axial flow, leading edge vortex, and trailing vortex) are presented, and the effects of external axial velocity and circulation gradients are investigated. The computations point to the controlling influence of the inner core flow on vortex behavior. They also confirm the existence of two particular critical swirl parameter values: S_0 , which separates vortex flow which decays smoothly from vortex flows which eventually "breaks down," and S_1 , the first singularity of the quasi-cylindrical system, at which point physical vortex breakdown is thought to occur. The results are close to the inviscid values for S_0 and $S_1[(2)^{1/2}$ and $3.8317/2$ for initially uniform axial flow].

I. Introduction

VORTEX flows exist in a bewildering variety of forms and are still only incompletely understood. The study of concentrated vortex flows suffers from a lack of analytical solutions which could serve as guidelines. Perplexing features such as vortex breakdown—the sudden expansion of vortex cores with possible stagnation and flow reversal on the axis appear under certain conditions. Earlier experimental and theoretical work in the area of concentrated vortex flows has been reviewed.¹

Laminar incompressible steady axisymmetric vortex flows are described by the corresponding form of the Navier-Stokes equations. These equations can be approximated by a parabolic viscous set, analogous to the boundary-layer equations, in regions where the stream surface angle remains small (quasi-cylindrical vortex flow), and by the inviscid equations

of rotating flow at and near the axis, and where stream surface angles become large (expansion or contraction of the core).²

Some solutions of the inviscid set pertaining to vortex flows at high swirl have been presented^{3,4}; here we shall now discuss a method of solving the parabolic viscous set and give corresponding results for different swirl parameters, initial velocity profiles, and external pressure and circulation gradients. Since the regions of validity of the two sets partially overlap on and near the axis, it should be possible to confirm some of the earlier results. The parabolic system has been used before in numerical computations by different methods.³⁻⁶ Gartshore⁴ and Mager⁶ each used a momentum-integral approach and encountered a singularity which they linked to the vortex breakdown phenomenon and to the critical swirl parameter $3.8317/2$ of flow in initially rigid rotation. The present results reinforce this view. Beyond this critical swirl ratio, Refs. 3 and 6 also obtained flows which contrasted in behavior with those below the critical swirl ratio.

The numerical method (N -parameter "exponential series integral method"†) to be used for the present study has pre-

Received August 31, 1970; revision received April 28, 1971. This work was partially supported by NASA Grant NGR 05-010-025.

Index category: Viscous Nonboundary-Layer Flows, Airplane and Component Aerodynamics.

* Associate Professor, Mechanical Engineering Department. Member AIAA.

† The term "integral method" is used here to avoid the cumbersome (but more accurate) terms "method of weighted residuals" or "method of integral relations."